Nuclear Instruments and Methods in Physics Research B xxx (2014) xxx–xxx

Contents lists available at ScienceDirect

Nuclear Instruments and Methods in Physics Research B

journal homepage: www.elsevier.com/locate/nimb

Generation of vacancy cluster-related defects during single MeV silicon ion implantation of silicon

Ž. Pastuović [a,*], I. Capan [b], R. Siegele [a], R. Jačimović [c], J. Forneris [d], D.D. Cohen [a], E. Vittone [d]

[a] Australian Nuclear Science and Technology Organization, Locked Bag 2001, Kirrawee DC NSW 2232, Australia
[b] Ruđer Bošković Institute, Bijenička cesta 54, P.O. Box 180, 10002 Zagreb, Croatia
[c] Jozef Stefan Institute, 1000 Ljubljana, Slovenia
[d] Physics Department and NIS Excellence Centre, University of Torino, INFN – sez. Torino, CNISM – sez. Torino, via P. Giuria 1, 10125 Torino, Italy

ARTICLE INFO

Article history:
Available online xxxx

Keywords:
Radiation damage
DLTS
Vacancy
Cluster
Single ion implantation

ABSTRACT

Deep Level Transient Spectroscopy (DLTS) has been used to study defects formed in bulk silicon after implantation of 8.3 MeV $^{28}Si^{3+}$ ions at room temperature. For this study, Schottky diodes prepared from *n*-type Czohralski-grown silicon wafers have been implanted in the single ion regime up to fluence value of 1×10^{10} cm^{-2} utilizing the scanning focused ion microbeam as implantation tool and the Ion Beam Induced Current (IBIC) technique for ion counting.

Differential DLTS analysis of the vacancy-rich region in self-implanted silicon reveals a formation of the broad vacancy-related defect state(s) at E_c −0.4 eV. Direct measurements of the electron capture kinetics associated with this trap at E_c −0.4 eV, prior to any annealing do not show an exponential behaviour typical for the simple point-like defects. The logarithmic capture kinetics is in accordance with the theory of majority carrier capture at extended or cluster-related defects. We have detected formation of two deep electron traps at E_c −0.56 eV and E_c −0.61 eV in the interstitial-rich region of the self-implanted silicon, before any annealing. No DLTS signal originating from vacancy-oxygen trap at E_c −0.17 eV, present in the sample irradiated with 0.8 MeV neutrons, has been recorded in the self-implanted sample.

1. Introduction

A new semiconductor device technology, providing better radiation hardness, is required for applications in high-energy physics, accelerator-based science, aerospace technology, i.e. the research communities developing and/or using semiconductor devices in harsh ionising radiation environments [1–5]. Novel devices are usually a result of complex manufacturing processes and therefore scarce and highly valuable [6,7]. Defect studies and radiation hardness testing procedures utilizing a low ionizing particle radiation provided by large accelerators or nuclear reactors usually require large particle fluences and corresponding long exposure times. A widely used alternative testing methodology utilizes a MeV ion beam irradiation to simulate radiation damage created by high energy neutrons, protons, pions, electrons, etc. With respect to low ionizing particles, ions having the energy per unit mass in 0.1–1 MeV/u range have the advantage of higher nuclear energy deposition per particle [8–10], thus creating comparable defect concentrations required for testing purposes at much lower fluence values and therefore at corresponding shorter exposure times. One major disadvantage of this approach is that the utilization of a broad ion beam requires the investigation of one test sample per each desired irradiation condition.

The capability of high-energy heavy-ion microprobes [11,12] to perform high-flux, high-frequency and high-precision scanning, compared to conventional ion broad-beam sources, offer advantages of: (a) selecting a particular region of interest on the device, (b) a computer controlled positioning of an ion micro-beam, (c) minimising irradiation area, (d) rapid irradiations, i.e. minimising exposure times and (e) single ion implantation.

The Ion Beam Induced Current (IBIC) is a mature and versatile ion microprobe technique for the characterisation of transport properties of charge carriers generated by single ions in active regions of semiconducting devices [13,14 and all Refs. therein].

We combine sub-micrometre ion beam sensitivity and IBIC technique for accurate implantation of desired number of ions in each pixel in order to create low level radiation damage in complex geometry patterns in simple planar test devices [15]. Each implanted ion dose is monitored *in vivo* by single ion counting, as well as the leakage current flowing in the IBIC sensing circuit. The total accumulated fluence from all irradiated areas is kept below

* Corresponding author. Tel.: +61 2 9717 3335; fax: +61 2 9717 3257.
E-mail address: zkp@ansto.gov.au (Ž. Pastuović).

http://dx.doi.org/10.1016/j.nimb.2014.02.082
0168-583X/

threshold for substantial leakage current increase. Each tested device, either micro-structured or having simple planar geometry, can be irradiated multiple times at different positions. The feasibility of this experimental protocol in the low radiation damage limit has already been demonstrated for testing and modelling of detrimental influence of energetic ions on the bulk properties of silicon [15–17] and diamond [7] used for fabrication of particle detectors. This protocol overcomes the previously discussed disadvantage of requiring a large number of test samples for different irradiation conditions. In order to justify its cost effectiveness in particular for novel detector radiation hardness testing, a similarity between defect states created by single heavy ion implantation and neutron (or high energy proton) irradiation of materials of interest should be demonstrated.

Vacancy-related defects are the most dominant electrically active defects in *n*-type silicon introduced by ion implantation. It is known that vacancy-related defects introduce three electronic states in the upper part of the band gap. Vacancy-oxygen (VO) pair, double negatively charge divacancy $V_2(=/-)$, and single negatively charge divacancy $V_2(-/0)$ are associated with levels at 0.18, 0.23 and 0.43 eV, respectively [18]. It has been observed that the divacancy has different behaviour when *n*-type Si is irradiated with electrons, neutrons or implanted with heavy ions [19]. Some studies report on creation of small vacancy and interstitial clusters with energy levels very close to single acceptor divacancy state energy [20]. So far our present knowledge on cluster-related defects and their properties, especially the carrier capture cross section, is very limited. Moreover, the structure of cluster-related defects and their influence on the charge carrier capture characteristics is not fully understood.

The aim of our studies is a better understanding of (i) the nature of defects created by single heavy ions at MeV energies and (ii) the influence of these electrically active defects on the charge carrier transport properties. In particular, the main objectives of this study are: (1) comparison of defect species created by single ion implantation and fast neutron irradiation (with maxima at 0.8 MeV) and (2) capture kinetics of created vacancy-related defects in silicon.

2. Experimental

n-Type silicon Schottky diodes were produced on phosphorus-doped (up to $1–2 \times 10^{14}$ cm^{-3}) Czohralski-grown (CZ) silicon crystal wafers with initial resistivities of 30 Ω cm. The Schottky barriers were formed by a thermal evaporation of gold at room temperature through a metal mask with a circular opening of 1 mm in diameter, while Ohmic contacts were formed by a thermal evaporation of aluminum on the back side of the silicon wafer. The quality of prepared diodes was characterized by *I–V* and *C–V* measurements at RT. The diode design (size, doping and thicknesses) and irradiation conditions have been optimised for (1) direct single ion detection utilizing IBIC technique and (2) DLTS analysis of the implanted samples. The samples were homogenously implanted by 8.3 MeV Si at the ANSTO heavy ion microprobe capable of focusing ions with the maximum rigidity of $ME/q^2 = 120$ [21]. The micro-beam with ion rate 2×10^{11} cm^{-2} s^{-1} was raster scanned multiple times over the total irradiated area of approximately 1 mm × 1 mm to avoid the instantaneous implantation of the full dose and achieve a more homogenous ion implantation. The scan area was divided in 512 × 512 pixels with a dwell time per pixel equal to 500 μs, i.e. on the average 5 ions were implanted in each pixel before the micro-beam was moved to the next pixel position. The total fluence was 10^{10} cm^{-2} with negligible error caused by a dead time of DAQ system.

The carousel facility of the 250 kW TRIGAMark II reactor at the Jozef Stefan Institute in Ljubljana was used for this work. The accumulated fluence of fast neutrons was 1×10^{12} cm^{-2}. Neutron irradiations were done inside a cadmium shield to filter out the thermal neutrons which would cause transmutation of the Si leaving only the fast neutrons to create damage in the samples.

Deep traps created in silicon were characterized using Deep Level Transient Spectroscopy (DLTS). The DLTS measurements were performed at temperatures between 80 and 300 K. To distinguish vacancy related defects which are created along the ion projectile cascade from defects related to mainly implanted ions and recoils (interstitials) created at and beyond the end of an ion range, depth profiling DLTS measurements [22] were performed at different reverse bias voltages and filling pulse amplitudes: (1) −2 to −0.2 V and (2) −5 to −3 V. Eight different rate windows from 0.5 to 50 ms were simultaneously obtained from one temperature scan in order to determine the DLTS signature of formed defects.

3. Results and discussion

The precise voltage settings required for DLTS experiment were chosen from the comparison of SRIM [23] simulations for the extent of disordered region dense with vacancies and interstitials following the single 8.3 MeV O ion implantation in silicon (Fig. 1) and *C–V* measurements (not shown). A reverse bias of −2 V with a fill pulse of −0.2 V sampled the vacancy-rich region corresponding to the implant tail, Fig. 1(c), while a reverse bias at −5 V with a fill pulse of −3 V sampled the interstitial-rich region close to implant peak, Fig. 1(b).

The measured free carrier concentration in the region of interest of pristine device is of the order of 10^{14} cm^{-3}. The cumulative decrease of the free carrier concentration in the irradiated device across the whole section from surface to the extent of implantation range (not shown) is supporting the fact that electron traps are formed within implantation range.

Fig. 2(a) show normalized DLTS spectra of the silicon ion implanted sample (Si:Si) and neutron irradiated sample (n:Si) measured at bias −5 V and rate window of 50 ms. Two electron traps with their maxima at about 97 and 188 K have been observed in the n:Si sample and three electron traps with their DLTS peak maxima at about 188, 232 and 258 K in the Si:Si sample for the rate window of 50 ms. These traps are referred to as E0–E3 in the following text. Activation energies of electron emission for the E0–E3 traps have been determined from Arrhenius plots of T^2-corrected electron emission rates as 0.17, 0.40, 0.56, and 0.61 eV, respectively.

Fig. 2(b) show differential DLTS spectra of the Si:Si sample measured for two different voltage settings (as described in the previous section) after implantation with no annealing carried out. The DLTS spectrum with the voltage setting sampling the vacancy-rich region (circles) resembles those reported in the literature for CZ Si crystals implanted with Si ions [18,24]. However, some unexpected features have been observed. A double acceptor state of divacancy $V_2(=/-)$ and vacancy-oxygen (VO) pair have not been detected at all in our DLTS measurement of the Si:Si sample. It has been reported in the literature that the intensity of $V_2(=/-)$ and VO is suppressed in heavy ion irradiated Si [25–27], but a complete lack of $V_2(=/-)$ and VO is a remarkable result. It should be pointed out, that Monakhov et al. [26] have used 6 MeV Si ions, while we have used 8.3 MeV ions. The suppression of VO and $V_2(=/-)$ defects is even more pronounced for 2 MeV Er ions implanted Si [22] and 46 MeV I ions implanted Si [25]. Moreover, despite the fact that we have used high energy ions, the DLTS peak ascribed to E1 defect is very sharp (typical for point-like defects), and notable, low-temperature broadening has not been observed as suggested elsewhere [27].

On the basis of a comparison of the measured trap parameters with the known values for defects induced by ion implantation

Please cite this article in press as: Ž. Pastuović et al., Generation of vacancy cluster-related defects during single MeV silicon ion implantation of silicon, Nucl. Instr. Meth. B (2014), http://dx.doi.org/10.1016/j.nimb.2014.02.082

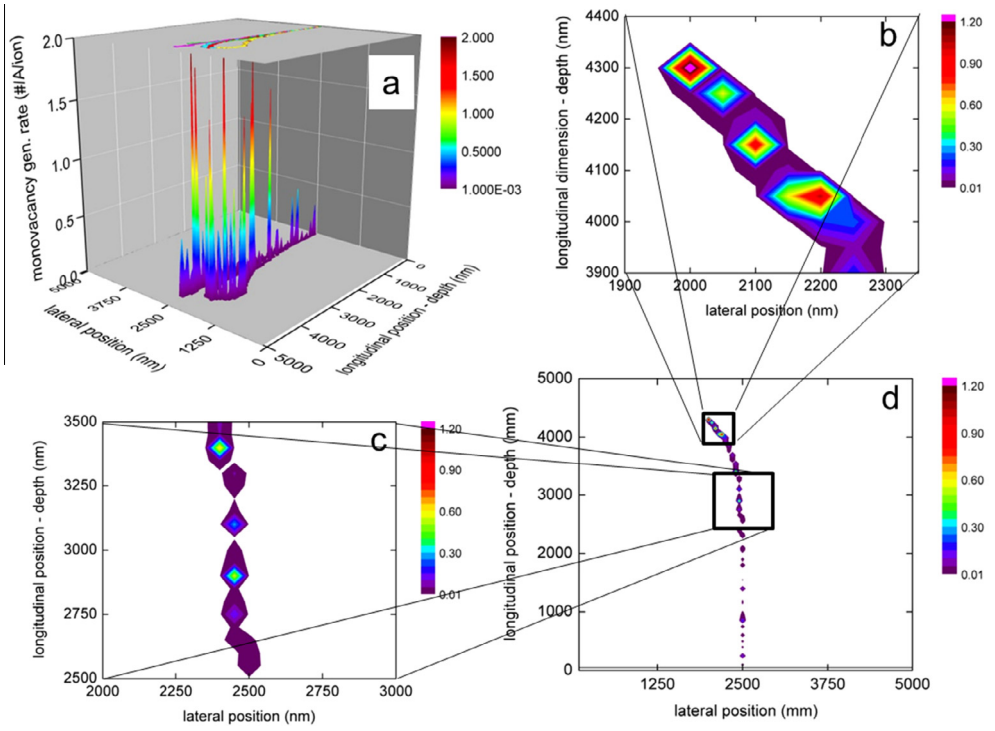

Fig. 1. Monte-Carlo simulation of the disordered region dense with primary defects following the single 8.3 MeV O ion implantation of silicon: (a) the cumulative projection on a horizontal beam plane of all monovacancies generated per unit length of a projectile (VGR) for five implanted ions with entry point at (2500,0) nm; (d) the surface contour plot of the VGR distribution generated by random chosen single ion cascade in material; (b) the enlarged disordered area close to the end of an ion range, and (c) the enlarged mid-range area corresponding to the implant tail. VGR yields shown by colour bars are expressed in monovacancy per Angstrom units. (For interpretation of the references to colour in this figure legend, the reader is referred to the web version of this article.)

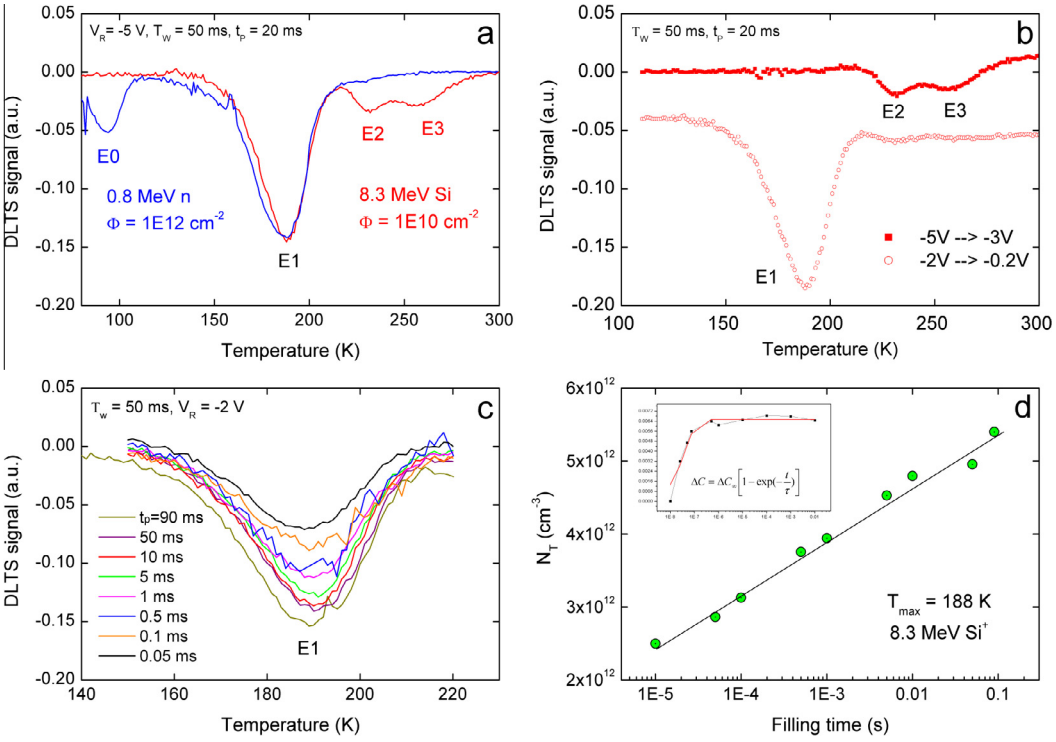

Fig. 2. Results of DLTS spectroscopy performed on implanted silicon diodes: (a) normalized DLTS spectra obtained by 8.3 MeV Si single ion implantation (red) and 0.8 MeV neutron irradiation (blue); (b) depth profiling of the vacancy-rich surface side of the implant tail (circles) and interstitial-rich region near the implant peak (squares) – off-set spectra are shown; (c) section of DLTS spectra corresponding to E1 trap formed in the implant tail as a function of the filling time (t_p); (d) results of carrier capture cross-section analysis of the E1 trap showing logarithmic behaviour typical for complex (cluster) defect structures. Inset in (d) shows the exponential dependence of carrier capture cross section typical for point defects. (For interpretation of the references to colour in this figure legend, the reader is referred to the web version of this article.)

Please cite this article in press as: Ž. Pastuović et al., Generation of vacancy cluster-related defects during single MeV silicon ion implantation of silicon, Nucl. Instr. Meth. B (2014), http://dx.doi.org/10.1016/j.nimb.2014.02.082

[16,24,28,29], we assign the E0 trap to vacancy-oxygen (VO) defect and the E1 trap to the (di)vacancy-related defect. As we have used the low phosphorous-doped silicon (doping at about 1–2×10^{14} cm^{-3}), the vacancy-phosphorous (VP) pair contribution to the overall E1 concentration calculated to be in the 10^{16} cm^{-3} range is neglected [30].

In some studies [24], E1 defect has been ascribed to the single acceptor state of divacancy. However, recent studies [18,19] have revealed more complex structure of those defects. Fleming et al. [19] have shown an unusual bistability of the divacancy-related defect in neutron, ion and high-energy electron damaged silicon. In their work, E4–E5 defects with energies at around 0.43 eV came from the most dominant single acceptor state of divacancy and its low-temperature shoulder. The discrepancy between intensities of two acceptor states of divacancy, and the broadening of the single acceptor state of divacancy has been detected only after neutron and ion irradiation [18].

In order to get more information regarding the nature of (di)-vacancy-related defect, the E1 trap, capture cross section measurements were performed. Fig. 2(c) shows the variation of the DLTS spectra originating from E1 state, dominantly created at the mid-range of implantation depth, sampled with increasing duration time of filling pulses. The most significant and well-documented difference between extended defects and point-like defects involves the logarithmic capture kinetics associated with extended defects. Such kinetics results from the Coulomb interaction between a charge carrier just being captured and other charges already captured at the defects [31]. Although sharpness of the DLTS peak corresponding to E1 traps is typical for point-like defects, Fig. 2(b), the capture cross section measurements have revealed a different nature for E1 trap. The fact that we have not observed any low-temperature broadening goes against the model which directly implies that, due to the lattice strain, the shallow state of the divacancy is not filled, as the strain introduces broadening [32].

Fig. 2(d) shows the resulting E1 trap concentration (N_T) as a function of the filling pulse duration. It is clear that filling time for the E1 trap increases and saturation is not observed. Moreover, the E1 trap clearly follows a logarithmic function of the filling pulse duration. At extended defects such as clusters and/or dislocations, a local space charge region that may affect charge capture is generated. In the model explained elsewhere [33], the capture kinetics is described by a time-dependent function for Coulomb potential, which reflects the number of charges captured at the extended defects. Therefore, the capture cross section becomes dependent upon the amount of charge already captured.

The displacement damage modelling of the implant tail region show increased vacancy density in disordered regions approximately 100 nm wide around individual ion-recoil cascades. Those regions have a high density of defects, mostly divacancy cluster-related defects. Although, according to our DLTS measurements inside those highly disordered regions only one mode of the divacancy exists (i.e. $V_2(-/0)$), it is possible that the existence of $V_2(=/-)$ state is completely suppressed, due to the charge compensation model [26]. The concentration of V_2 traps in the disordered region exceeds the doping concentration. The single acceptor state of divacancy, $V_2(-/0)$, is being filled up during the filling pulse in the DLTS measurements because of the carrier diffusion into the disordered region. As a result, the supply of free electrons is exhausted even before the occupancy of the $V_2(-/0)$ trap reaches a saturation, Fig. 2(d), and the occupancy of the shallower $V_2(=/-)$ states is negligible, giving no response during DLTS measurement. Taking into account all results and simulations, we can assign the E1 trap to the closely spaced divacancies which are formed directly from the nearest neighbour monovacancies originating from the single ion impact cascade.

We shall now briefly return to Fig. 2(b) and DLTS spectrum with the voltage settings sampling the interstitial-rich region. We have detected two small, closely spaced broad peaks. The origin of those very deep defects is not clear. They resemble those reported in the literature for ion implanted silicon [34]. Benton et al. have used 145 keV–1.2 MeV Si ions to doses of 1×10^{10}–5×10^{13} cm^{-2} and annealed their samples at 450–750 °C and ascribed those defects to intrinsic, cluster-related defects. Although at the same dose, we have used substantially higher beam energies (8.3 MeV) and no annealing has been performed upon implantation. Privitera et al. [35] demonstrated room-temperature migration of Si interstitials over several microns beyond ion implantation depth. Similarly, Larsen et al. [36] in a study of migration of Si interstitials at room temperature using a spreading resistance technique, detected dopant deactivation up to a depth of several microns beyond the region directly modified by implanted ions. In their transient spectroscopy studies Giri et al. [37] observed a newly found level labelled as D1 with the activation energy in the 0.49–0.56 eV range and an approximate capture cross section of 1×10^{-15} cm^{-2} in as-implanted samples. Similarly to our results, they also observed moderate energy broadening of D1 peak. The sensitivity of the activation energy to ion type and radiation dose indicates the influence of changes in the environment of the defect in the damaged layer. The cluster binding energy is known to change with the size of clusters [38] and this might be reflected in the activation energy of the associated defect. Moreover, it has been reported that the photoluminescence line, W, due to very small interstitial silicon cluster, is present in the interstitial-rich region of ion implanted silicon, before any annealing [39]. Therefore it appears reasonable to conclude that E2 and E3, which lie deep in the gap, are interstitial clusters-related defects. However, further detailed studies are needed in order to fully understand the behaviour of interstitial-related clusters.

4. Conclusion

A depth profiling of partly damaged silicon layer implanted with scanned 8.3 MeV Si ion microbeam has been performed by means of DLTS measurements at two different voltage settings, in order to distinguish defects which are created in the vacancy-rich and interstitial-rich regions. DLTS analysis of the vacancy-rich region in self-implanted silicon reveals a formation of the vacancy-related defect(s) with activation energy at $E_c - 0.4$ eV. Direct measurement of the electron capture kinetics associated with these states, prior to any annealing, does not show the exponential behaviour typical for simple point defects. The logarithmic capture kinetics is in accordance with the theory of majority carrier capture at extended or cluster-related defects. Our DLTS results suggest that small clusters of $V_2(-/0)$ defects with activation energy close to $E_c - 0.4$ eV are created in the highly disordered regions of silicon before any annealing. Complete suppression of the VO and $V_2(=/-)$ states in DLTS results is interpreted according to the model of local compensation of the carrier concentration in highly disordered regions located within the ion cascade region.

Acknowledgements

The authors wish to acknowledge the support of the ANSTO Accelerator Science Project No. 0208 and the IAEA under the CRP project F11016.

References

[1] F. Gianotti, M.L. Mangano, T. Virdee, et al., Eur. Phys. J. C 39 (2005) 293–333.
[2] E. Fretwurst et al., CERN RD-50 collaboration, Nucl. Instr. Meth. A 552 (2005) 7.
[3] G. Casse, Nucl. Instr. Meth. A 598 (2009) 54.

Please cite this article in press as: Ž. Pastuović et al., Generation of vacancy cluster-related defects during single MeV silicon ion implantation of silicon, Nucl. Instr. Meth. B (2014), http://dx.doi.org/10.1016/j.nimb.2014.02.082

[4] Y. Unno, Nucl. Instr. Meth. A 612 (2010) 439.
[5] D. Bortoletto, Nucl. Instr. Meth. A 623 (2010) 35.
[6] D. Asner et al., CERN RD42 collaboration, Nucl. Instr. Meth. A 636 (2011) S125.
[7] I. Zamboni, Z. Pastuovic, M. Jaksic, Diamond Relat. Mater. 31 (2013) 65.
[8] G.P. Summers, E.A. Burke, P. Shapiro, S.R. Messenger, R.J. Walters, IEEE Trans. Nucl. Sci. 40 (6) (1993) 1372.
[9] S.R. Messenger, E.A. Burke, G.P. Summers, M.A. Xapsos, R.J. Walters, E.M. Jackson, B.D. Weaver, IEEE Trans. Nucl. Sci. 46 (6) (1999) 1595.
[10] A. Chilingarov, D. Lipka, J.S. Meyer, T. Sloan, Nucl. Instr. Meth. A 449 (2000) 277.
[11] R. Siegele, A.G. Kachenko, M. Ionescu, D.D. Cohen, Nucl. Instr. Meth. B 267 (2009) 2054.
[12] M. Jaksic et al., Nucl. Instr. Meth. B 260 (2007) 114.
[13] M.B.H. Breese, E. Vittone, G. Vizkelethy, P.J. Sellin, Nucl. Instr. Meth. B 264 (2007) 345.
[14] E. Vittone, Z. Pastuovic, P. Olivero, C. Manfredotti, M. Jaksic, A. Lo Giudice, F. Fizzotti, E. Colombo, Nucl. Instr. Meth. B 266 (2008) 1312.
[15] Z. Pastuovic, M. Jaksic, G. Kalinka, M. Novak, A. Simon, IEEE Trans. Nucl. Sci. 56 (2009) 2457.
[16] Z. Pastuovic, E. Vittone, I. Capan, M. Jaksic, Appl. Phys. Lett. 98 (2011) 091201.
[17] G. Vizkelethy, R.M. Fleming, E. Bielejec, Nucl. Instr. Meth. B 306 (2013) 176.
[18] I. Kovacevic, V.P. Markevich, I.D. Hawkins, B. Pivac, A.R. Peaker, J. Phys.: Condens. Matter 17 (2005) S2229.
[19] R.M. Fleming, C.H. Seager, D.V. Lang, E. Bilejec, J.M. Campbell, J. Appl. Phys. 104 (2008) 083702.
[20] D.A. Abdulmalik, P.G. Coleman, I.Y. Al-Qaradawi, Appl. Surf. Sci. 252 (2006) 3209.
[21] R. Siegele, D. Cohen, N. Dytlewski, Nucl. Instr. Meth. Phys. Res. B 158 (1999) 31.
[22] P. Leveque, H. Kortegaard Nielsen, P. Pellegrino, A. Hallen, B.G. Svensson, A.Yu. Kuznetsov, J. Wong-Leung, C. Jagadish, V. Privitera, J. Appl. Phys. 93 (2003) 5118.
[23] Available at: <http://www.srim.org>.
[24] A. Hallen, N. Keskilato, Nucl. Instr. Meth. B 186 (2002) 41.
[25] L. Vines, E.V. Monakhov, J. Jensen, A.Yu. Kuznetsov, B.G. Svensson, Phys. Rev. B 79 (2009) 075206.
[26] E.V. Monakhov, J. Wong-Leung, A.Yu. Kuznetsov, C. Jagadish, B.G. Svensson, Phys. Rev. B 65 (2002) 245201.
[27] B.G. Svensson, C. Jagadish, A. Hallen, J. Lalita, Phys. Rev. B 55 (1997) 10498.
[28] A. Junkes, D. Eckstein, I. Pintilie, L.F. Makarenko, E. Fretwurst, Nucl. Instr. Meth. A 612 (2010) 525.
[29] A.R. Peaker, J.H. Evans-Freeman, P.Y.Y. Kan, I.D. Hawkins, J. Terry, C. Jeynes, L. Rubaldo, Mater. Sci. Eng. B71 (2000) 143.
[30] G.D. Watkins, J.W. Corbett, Phys. Rev. 134 (5A) (1964) A1359.
[31] O. Yastrubchak, T. Wosinski, A. Makosa, T. Figielski, A.L. Toth, Physica B 308–310 (2001) 757.
[32] B.G. Svensson, B. Mohadjeri, A. Hallen, J.H. Svensson, J.W. Corbett, Phys. Rev. B 43 (1991) 2292.
[33] I. Capan, V. Borjanovic, B. Pivac, Sol. Energy Mater. Sol. Cells 91 (2007) 931.
[34] J.L. Benton, S. Libertino, P. Kringhoy, D.J. Eaglesham, J.M. Poate, S. Coffa, J. Appl. Phys. 82 (1) (1997) 120.
[35] V. Privitera, S. Coffa, F. Priolo, K. Kyllesbech Larsen, G. Mannino, Appl. Phys. Lett. 68 (1996) 3422.
[36] K. Kyllesbech Larsen, V. Privitera, S. Coffa, F. Priolo, S. Campisano, A. Carnera, Phys. Rev. Lett. 76 (1996) 1493.
[37] P.K. Giri, Y.N. Mohapatra, J. Appl. Phys. 84 (1998) 1901.
[38] J. Kim, F. Kirchhoff, W.G. Aulbur, J.W. Wilkins, Phys. Rev. Lett. 83 (1999) 1990.
[39] R. Jones, A.G. Eberlein, N. Pinho, B.J. Coomer, J.P. Goss, P.R. Briddon, S. Öberg, Nucl. Instr. Meth. B 186 (2002) 10.

Please cite this article in press as: Ž. Pastuović et al., Generation of vacancy cluster-related defects during single MeV silicon ion implantation of silicon, Nucl. Instr. Meth. B (2014), http://dx.doi.org/10.1016/j.nimb.2014.02.082